  DOI 10.1515/HTMP.2011.012

Pin-On-Disc Characterization of Brass/Ferritic and Pearlitic Ductile Iron Rubbing Pair

Melik Çetin[1,*]

[1] Karabuk University, Technical Education Faculty, Division of Metal Casting, Karabuk, Turkey

Abstract. Wear behaviour of special brass produced through two different methods (centrifugal and sand casting) was investigated. The wear tests were carried out at sliding velocities of 0.2 $m\,s^{-1}$, 0.3 $m\,s^{-1}$, 0.4 $m\,s^{-1}$ and 0.5 $m\,s^{-1}$ and under 10 N, 20 N, and 40 N variable loads. The sliding distance was 600 m for all the tests. A pin-on-disc device with round specimen inserts was used to conduct friction and wear tests in which the friction coefficient, the contact temperature and the linear wear of the tribo-pairs were continuously recorded against sliding distance. Two different materials were used as the counterparts, namely ferritic ductile iron equivalent to GGG40 and pearlitic ductile iron equivalent to GGG60. The microstructures and wear scars of the brass specimens were examined by optical, scanning electron microscopy (SEM) and X-ray microanalyses by EDAX. A correlation between hardness and wear volume rate was established for the investigated centrifugally cast and sand cast brass specimens. The volume rate of specimens produced by sand casting method was generally found to be higher than those of centrifugally cast specimens. Ferritic ductile counterpart led to higher wear volume rate than pearlitic ductile counterpart for the both specimens. Severe abrasive wear scars were observed for the sand cast specimens/ferritic ductile iron pair. However, severe adhesive wear took place for the centrifugally cast specimen/pearlitic ductile iron pair.

Keywords. Wear, brass, centrifugal casting, sand casting, pearlitic ductile iron, ferritic ductile iron.

1 Introduction

Brass is a material widely used in friction parts of machines, as bearing liners, bushing, etc. Properties such as high strength and ductility, fatigue strength, wear resistance are necessary for this material, and it is important to understand microstructural changes during its service life [1–3]. For many applications, brass is usually the first choice of materials for household devices, electrical and all precision engineering industries [4].

In the automobile industry, particularly in the manufacturing of components, where resistance to wear is the chief requirement, high-strength brasses are commonly used. High-strength brasses are suitable mainly for engineering areas where high strength to support heavy loads and/or high resistance to wear and corrosion are required. The main advantages of high-strength brasses are further improvement of mechanical properties by heat treatment as well as their low cost [5–8].

Brass alloys having a higher Zn content contain both α and β phases at room temperature. The β phase has an ordered bcc crystal structure and is harder and stronger than α phase; consequently, $\alpha + \beta$ alloys are generally hot worked [4]. High-strength brasses can be mainly classified as $\alpha + \beta$ or β brasses, containing the alloying elements such as aluminium, silicon, manganese, etc. [8]. Aluminium raises the corrosion resistance of brasses by forming a protective Al_2O_3 oxide film on their surfaces. Iron is practically insoluble in the α and β phases and is only present in the form of silicides. Iron particles increase the formation rate of nucleation and recrystallization and delay the following grain growth. Silicon enhances the corrosion resistance, wear resistance (due to silicide formation), and workability of brasses. Manganese increases the ultimate tensile strength, ductility, and wear resistance of the brasses. Nickel reduces the tendency of the brasses to corrosion cracking. Lead is particular alloying element, since it precipitates along boundaries as low-melting-temperature layer and results in the hot-shortness of the brasses.

Brass is widely used for production of bearing materials in industrial service. The heads of rolls made of ductile iron used in rolling mills rotate in brass bearing. A thorough review has been made of previous work concerning the parameters on the wear characteristics of extruded brass against steel disc used as counter abrader [2, 3, 6–10]. Most of the investigations were concerned with the identification of a change in the resulting heat treatment, environments and composition of brass [6–10]. There is little published work concerning the effects of the casting parameters on wear characteristics [6]. Also, most of the previous work was carried out against steel disc as counter abrader materials [1–13]. However, adequate data is not available on

Corresponding author: Melik Çetin, Karabuk University, Technical Education Faculty, Division of Metal Casting, 78100 Karabuk, Turkey; E-mail: mcetin@karabuk.edu.tr.

Received: September 1, 2010. Accepted: October 6, 2010.

Cu	Zn	Al	Fe	Pb	Mn	Sn	Si	Ni	Sb
62.95	31.72	2.55	0.64	0.96	0.31	0.49	0.26	0.07	0.064

Table 1.

the brass materials produced by centrifugal casting and sand casting methods. Similarly, adequate work is not available for ferritic and pearlitic ductile iron disc materials.

The aim of this study is to establish relationship between wear parameters and material properties of special brasses which were produced through centrifugal casting and sand casting methods. Also, the influence of ferritic and pearlitic ductile iron counterpart materials on wear volume rate was aimed to be established.

2 Experimental Procedure

2.1 Material Production

Copper-zinc alloy was melted in a graphite crucible. The molten alloys were poured from temperatures approximately 323 K above their liquidus temperature into green sand and centrifugal casting moulds. Prior to centrifugal casting, the mould was pre-heated to 523 K. The molten copper-zinc alloys were poured into a horizontal centrifugal casting machine rotating at 1000 rpm. The outer diameter of the cylindrical casting was 120 mm, the wall thickness was 15 mm, and the length of the casting was 900 mm. The chemical composition of copper-zinc alloys is given in Table 1.

For optical microscopy examination, standard metallographic procedure was applied to the specimens (grinding, polishing and etching in a solution of 1 g $FeCl_3$ and 20 ml HCl in 100 ml water). In the present work, optical microscopy examination of the specimens was carried out using a Nikon DIC optical microscope. The grain size measurements were also carried out using MSQ Plus 6.5 type Image analyser. The worn surfaces all of the wear specimens were examined by SEM and EDAX.

2.2 Measurement of Density, Hardness and Tensile Properties

Hardness measurements were made in universal AFFRI hardness measurement equipment (HV5). For each specimen, five hardness measurements were carried out. Density measurement was also carried out on the specimens. Water displacement technique was adopted for measuring density. A Mettler microbalance was used for weighting the specimens for the density measurement. Tensile strength and elongation of 4 mm gauge diameter, 20 mm gauge lenth specimens were determined using a Shimadzu universal testing machine at a strain rate of 2 mm/min at ambient temperature. The reported values of the properties represent an average of three measurements.

2.3 Wear Tests

Dry sliding wear tests were performed using a pin-on-disc type wear test machine shown in Figure 1. The test materials in the form of pins of 6.25 mm in diameter and 50 mm in length were made to slide against a as-cast ferritic ductile iron disc (3.2 % C, 2.8 % Si, 0.27 % Mn, 0.023 % P, 0.017 % S, 0.04 % Mg) and as-cast pearlitic ductile iron disc (3.2 % C, 2.8 % Si, 0.32 % Mn, 1.41 % Cu, 0.021 % P, 0.015 % S, 0.03 % Mg). The hardness values of ferritic and pearlitic discs were 190 and 220 HB, respectively. The mean diameter of the discs was approximately at 90 mm. The disc was ground to a surface finish of approximately 0.15 μm (CLA). The wear tests were carried out at four different sliding speeds of 0.2 m s^{-1}, 0.3 m s^{-1}, 0.4 m s^{-1} and 0.5 m s^{-1} under the loads of 10 N, 20 N and 40 N and sliding distance of 600 m, in the atmospheric condition with the relative humidity of 54 % and temperature of 296 K. The experimental data, i.e. coefficient of friction and time, were recorded continuously during the wear tests. The contact temperature was measured using a chromel-alumel type thermocouple inserted into a 1.5 mm diameter hole, 2 mm back from contacting surfaces monitoring the temperature near surface of the specimen during the wear tests (Figure 2). Prior to testing, test specimens were ground against 800 grit SiC paper, and then cleaned in acetone, dried and then weighed using an electronic balance having an accuracy of 0.1 mg. The specimens were then placed into the wear test machine and the sliding wear tests were carried out at different sliding speeds and loads. After each test, the specimen was removed, ultrasonically cleaned in acetone and weighed. At each load, the volume losses from the surface of specimens were determined as a function of sliding distance, sliding velocity, and applied load.

The wear rate is defined as the volume loss, V, divided by the sliding distance, L

$$K = V/L,$$

Where K has the units of volume loss per unit distance (mm^3/m).

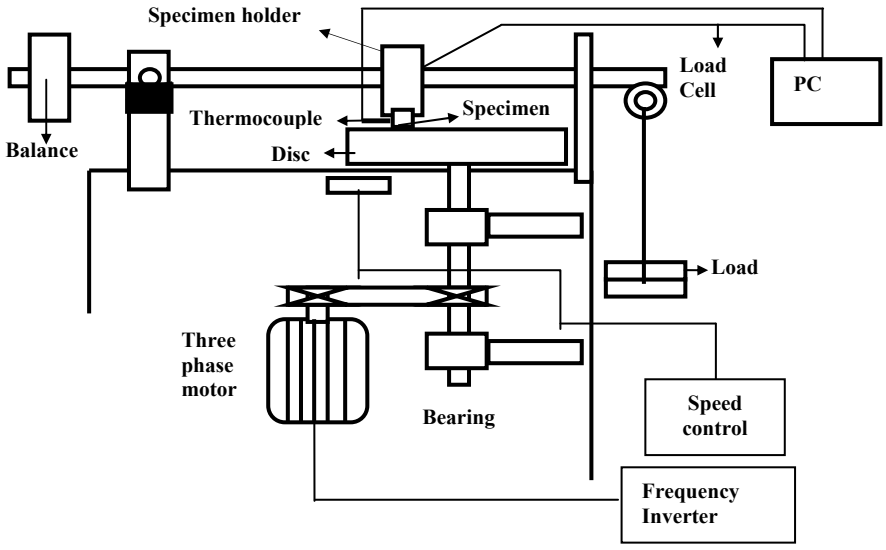

Figure 1. Pin-on-disc wear tester

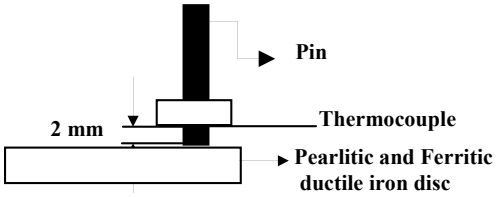

Figure 2. The position of the thermocouple in the brass pin.

3 Results and Discussions

3.1 Microstructure Evaluation

Figure 3 shows the microstructures of the brass produced by sand casting and centrifugal casting methods. It can be seen that needle like grains of sand cast specimens are larger than those of the centrifugally cast specimens. Actually, the cooling rate of cast specimen affects its microstructure, quality, and properties. The structure of sand cast specimen, often large with thick walls, may be the result of slow cooling. This increases the grain size and leads to a coarse microstructure (Figure 3(a)). Coarse grains can allow elements of an alloy to separate, which also decreases mechanical properties of casting. Conversely, centrifugally cast parts (metal mould) generally cool more quickly and results in microstructure with fine grains (Figure 3(b)) having less alloy segregation. Microscopic examinations revealed that light coloured needle like α-phase precipitated in dark coloured β-phase matrix in the microstructures. Also, there are grey coloured areas in the microstructure. Some researches [5–7] reported that Mn_5Si_3 intermetallics in microstructure are grey in colour. Also, Figure 3 shows that the amount of porosity is higher in the sand cast microstructure near the outer periphery when compared to that in the centrifugally cast microstructure. During centrifugal casting, gas bubbles also move to the inner periphery due to their lower density than the density of copper melts and results in a dense microstructure. This is also supported by the density results in Table 2. Another advantage of centrifugal casting technique is its ability to distribute the particles present in the matrix. The resulting microstructure of the centrifugally cast parts depends on various factor such as rotational speed of the mould and its size, the volume fraction of the particles and mould pre-heat temperature.

3.2 Density, Hardness, Tensile Strength and Elongation

Table 2 shows the density, hardness, tensile strength and elongation of the both specimens. The results indicate that the centrifugal casting led to higher density, hardness, ultimate tensile strength and elongation when compared to the sand casting. The increase in the density, hardness, strength and elongation were caused by the decrease in porosity in the centrifugally cast brass. Centrifugally cast parts (metal mould) generally cool more quickly and results in microstructure with smaller grains (Figure 3) having less alloy segregation and higher density, hardness, strength and elongation when compared to the sand cast parts (Table 2).

3.3 Wear Behaviour

Figure 4 shows the effect of applied load on the wear volume rate of the both materials against pearlitic ductile iron disc under the loads of 10 N, 20 N and 40 N and at 0.2 $m\,s^{-1}$, 0.3 $m\,s^{-1}$, 0.4 $m\,s^{-1}$and 0.5 $m\,s^{-1}$ sliding speeds. At all the sliding speeds, the wear volume rate of the both materials decrease with increasing the applied

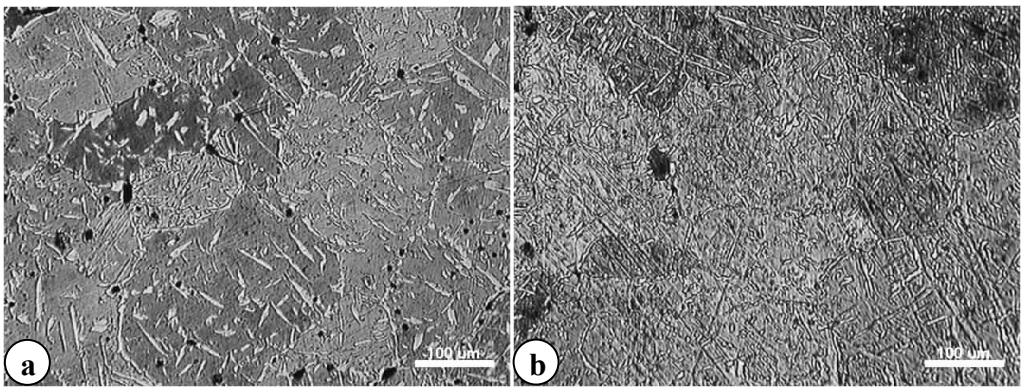

Figure 3. Microstructure of the specimens (a) sand casting (b) centrifugally casting.

Production methods	Density (Mg/m^3)	Hardness (HV5)	UTS (MPa)	Elongation (%)
Centrifugally casting	8.045	205	500	6.65
Sand casting	7.6730	175	225	2.81

Table 2.

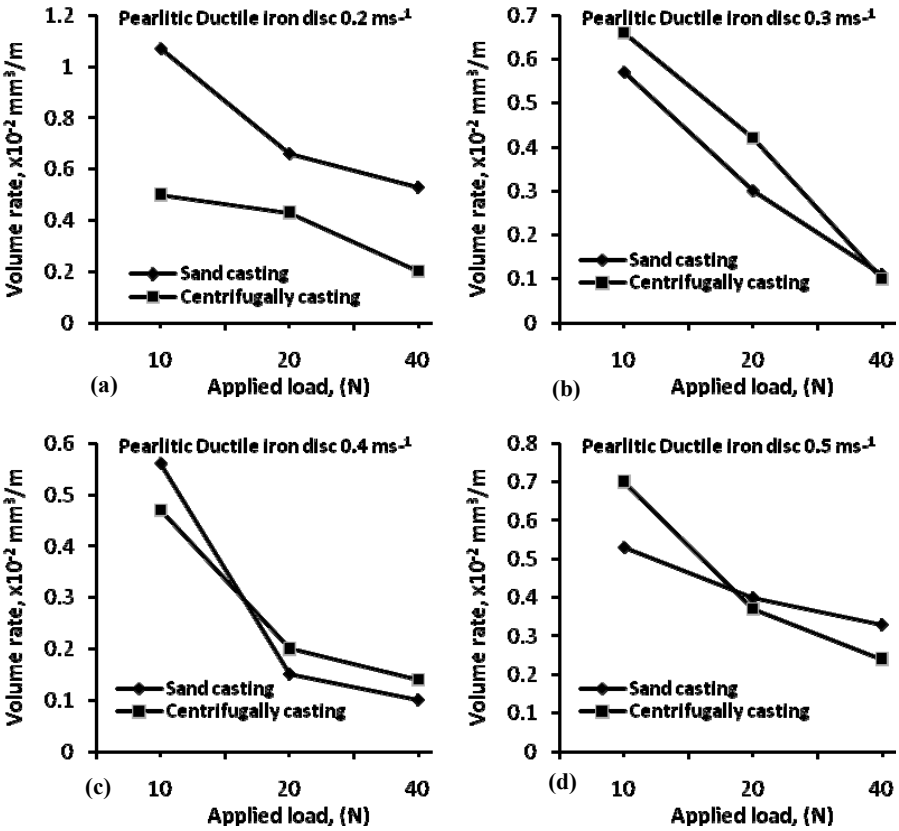

Figure 4. Variation of volume rate vs. applied loads at constant sliding distance (600 m) and different sliding speed (a) 0.2 m s^{-1}, (b) 0.3 m s^{-1}, (c) 0.4 m s^{-1} and (d) 0.5 m s^{-1} for pearlitic ductile iron disc.

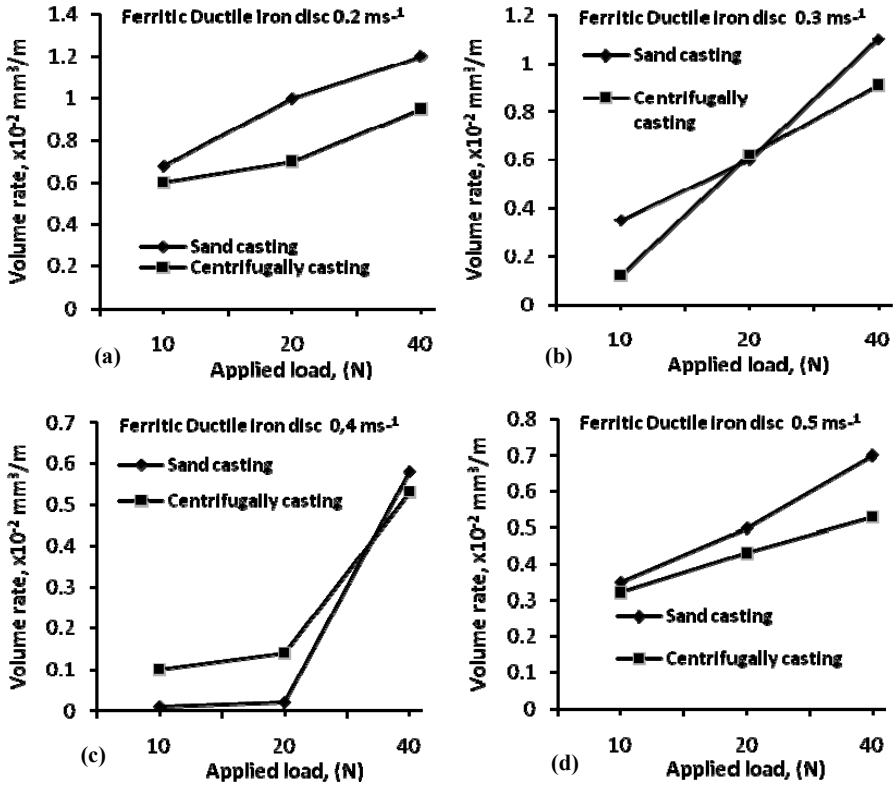

Figure 5. Variation of volume rate vs. applied loads at constant sliding distance (600 m) and different sliding speed (a) 0.2 m s^{-1}, (b) 0.3 m s^{-1}, (c) 0.4 m s^{-1} and (d) 0.5 m s^{-1} for ferritic ductile iron disc.

load (Figure 4(a)–(d)). However, the decrease in the wear volume rate is slower at the sliding speeds of 0.2 m s^{-1} and 0.5 m s^{-1} than at the sliding speeds of 0.3 m s^{-1} and 0.4 m s^{-1}. Figure 4 also indicates that at all the sliding speeds, centrifugally cast specimens show lower wear volume rate than the sand cast specimens.

On the other hand, Figure 5 shows the effect of applied load on the wear volume rate of the both materials against ferritic ductile iron disc. It was found that at all the sliding speeds, wear volume rate of the sand and centrifugally cast specimens increase with increasing the applied loads of 10 N, 20 N and 40 N for the ferritic ductile iron disc (Figure 5(a)–(d)). The centrifugally cast specimens show lower wear volume rate than the sand cast specimens under the loads of 10–40 N for all the sliding speeds (Figure 5(a)–(d)).

The centrifugally cast specimens, which are harder than the sand cast specimens as shown in Table 2, show lower wear volume rates. The wear volume rate-hardness relationship in Figure 4 and Table 2 exhibits that wear volume rate under all the applied loads and at all the sliding speeds decreases with the increase in hardness from 175 to 205 HV_5 for the pearlitic ductile iron disc. However, wear volume rate-hardness relationship in Figure 5 and Table 2 exhibits that wear volume rate under all the applied loads and at all the sliding speed increases with the increase in hardness from 175 to 205 HV_5 for the ferritic ductile iron disc. Moreover, the effect of applied load on wear volume rate becomes more prevailing at higher loads. In general, the weight loss of the pin materials increases linearly with increasing sliding distance and applied load. Since wear rate is the ratio of wear volume to sliding distance in a certain wear condition, wear rate decreased with increasing sliding distance, although weight loss increased with increasing sliding distance. Feyzullahoglu et al. [11] observed that for WM-2, WM-5 and CW619 brasses, weight loss increases linearly up to a certain sliding distance and attains a maximum value for 115 N applied load, but with further increase in sliding distance weight loss has a decreasing trend. The centrifugally cast brass is harder than the sand cast brass (Table 2) and for that reason, wear volume rate of the centrifugally cast brass is lower than that of sand cast brass (Figure 4(a)–(d) and Figure 5(a)–(d)) for the both counterpart. Wear of brass material depends on hardness of the alloy, α and β phases present in microstructures and the alloying elements (especially Al and Mn) [6, 8]. Previous studies also report the reduction in wear rate with increasing materials hardness. Wear of materials is, to a certain extent, directly connected with hardness and matrix structure [12,13]. Harder materials have comparatively low wear

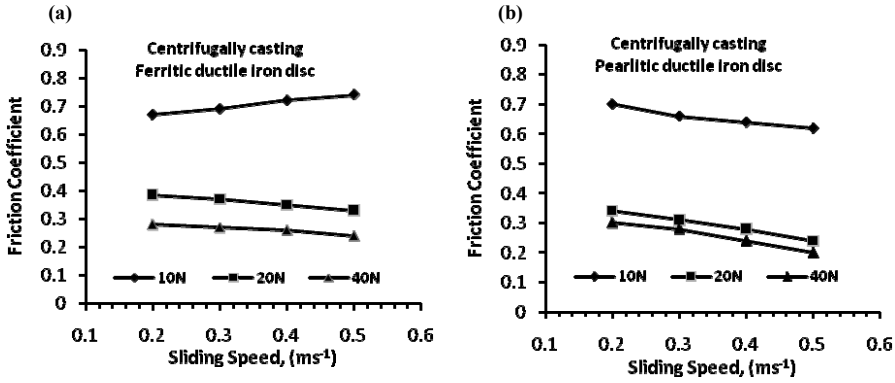

Figure 6. Variation of friction coefficient as a function of sliding speed at different loads and constant sliding distance (600 m) for centrifugally casting (a) ferritic ductile iron disc; (b) pearlitic ductile iron disc.

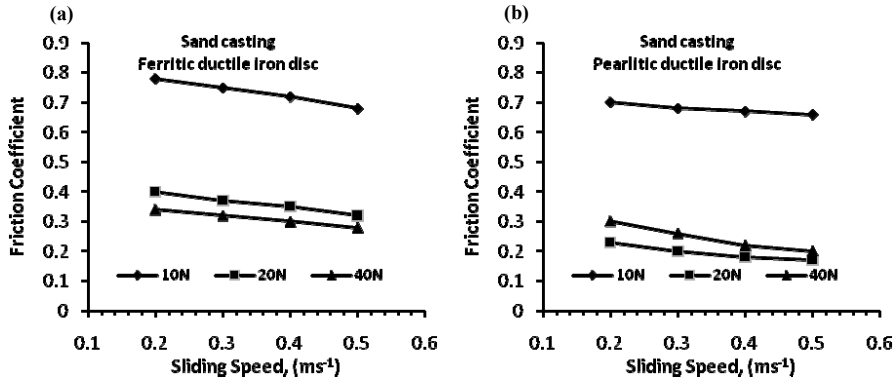

Figure 7. Variation of friction coefficient as a function of sliding speed at different loads and constant sliding distance (600 m) for sand casting (a) ferritic ductile iron disc; (b) pearlitic ductile iron disc.

rate, and the results presented here are consistent with this fact. In general, wear resistance of a material is proportional to its hardness [14]. As presented in Table 2, the wear volume rate of centrifugally cast brass specimen's decreases with increasing hardness (Figure 4 and Figure 5). In consistent with the wear results (Figure 4 and Figure 5), the wear volume rate of the centrifugally and sand cast specimens is lower for pearlitic ductile iron counterpart when compared to ferritic ductile iron counterparts at all the sliding speeds.

The friction coefficient for both specimens was also determined. The results are given in Figure 6 and Figure 7. The variation of the friction coefficient with the applied load is also presented in Figure 6 and Figure 7. It is seen from the results that friction coefficient generally decreases with increasing sliding speed and the applied load. W. X. Qi et al. also reported similar finding in the wear of Cu-Cr-Zr alloy [15]. The reduction of the friction coefficient with increased load and speed was attributed to the formation of oxide film on worn surface [16]. Figure 6 shows that the friction coefficient of centrifugally cast specimens decreases under the applied loads of 20 and 40 N while it increases under the applied load of 10 N and exhibit a nearly linear relationship for ferritic ductile iron disc. On the other hand, the friction coefficient of centrifugally cast specimens decreases with the sliding speed in the ranges between 0.2–0.5 m s^{-1} at all the applied load. Against the pearlitic ductile iron disc, the centrifugally cast specimens have lower friction coefficient than the sand cast specimens.

Contact temperature variation during the sliding of centrifugally cast and sand cast specimens with constant sliding distance at different sliding speeds and under the load 40 N is shown in Figure 8 and Figure 9 for the both discs. Figure 8 and Figure 9 show two different trends of variation in temperature with sliding distances at different speeds of sliding. At low sliding speed (0.2 m s^{-1}), four regimes of temperature variation with sliding distances are observed, whereas at high sliding speed two regimes of temperature variation are observed. Out of the two regimes of temperature variation with sliding distance at 0.3, 0.4 and 0.5 m s^{-1} speeds, the first one corresponds to initial steep rise in temperature during the run, and the second one corresponds to steady state temperature. Centrifugally cast specimen has shown this tendency (two regimes) throughout the entire sliding at 0.2 m s^{-1} speeds (Figure 8(a) and Figure 9(a)). Four regimes of temperature variation with sliding distance (Figure 8(a)) are observed at 0.5 m s^{-1} and 0.2 m s^{-1} slid-

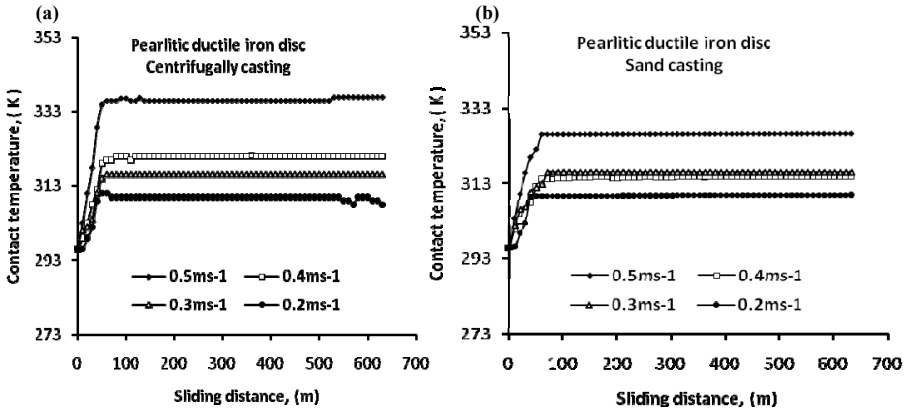

Figure 8. Evolution of the contact temperature (T in K) with sliding distance in different liner sliding speed for 40 N applied load.

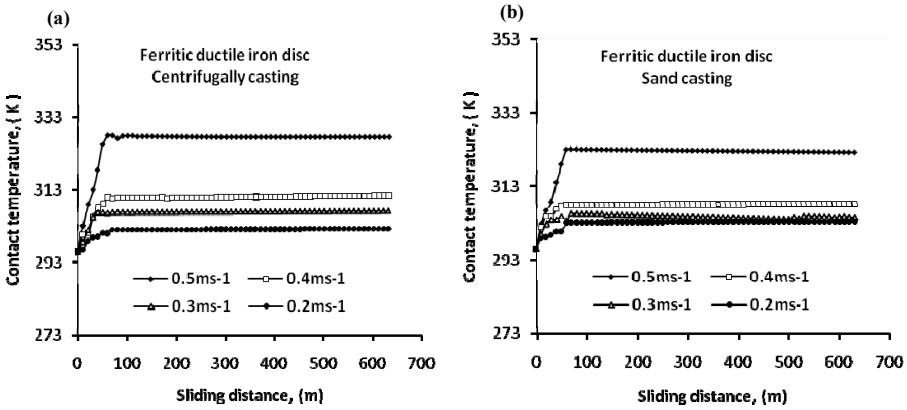

Figure 9. Evolution of the contact tempereture with sliding distance in different liner sliding speed for 40 N applied load.

ing speeds. Two regimes of temperature variation were observed for only sand cast brass specimens for the both discs. The contact temperature increased with the sliding speed. The gradient of temperature increment is maximum at the beginning of sliding at 0.5 m s^{-1} sliding speed for the centrifugally cast and sand cast brasses for all wear conditions (Figure 8 and Figure 9). It gradually increases with sliding distance. However, at 0.2 m s^{-1}, 0.3 m s^{-1} and 0.4 m s^{-1} sliding speeds, the contact temperature increase with the initial steep run and this increment remains stable from beginning until 600 m sliding distance; this can be attributed to the hard adhesive wear and the repeated contact of the same junctions. In consistent with the wear results (Figure 4 and Figure 5), the wear volume rate of the centrifugally cast and sand cast brass specimens is lower for the pearlitic ductile iron disc while both brass specimens show higher wear volume rate for ferritic ductile iron disc. This might be due to the low frictional heat on low hardness ferritic ductile iron disc in dry sliding condition. In the case of low temperature, oxide formation decreases and this, in turn, increases the wear volume rate. Generally, the wear volume rate, friction coefficients and contact temperature of specimens that was tested on the pearlitic ductile iron disc were found to be lower than those tested on the ferritic ductile iron disc (Figures 4–9).

Figures 10, 11 and 12 show the SEM photographs of the specimens taken from the surface of the sand cast and centrifugally cast brasses worn against the pearlitic and ferritic ductile iron disc at the sliding speeds of 0.2 m s^{-1} 0.3 m s^{-1}, 0.4 m s^{-1} and 0.5 m s^{-1}. Visual examination of the worn surfaces indicates that wear tests lead to rough surfaces. This is also evident in Figure 10 and Figure 11 with wide and deep grooves. During the tests, wear is progressed by ploughing action of the pearlitic ductile iron disc by forming grooves in the wear tracks aligned parallel to the sliding directions. This indicates the abrasive wear mechanism. In some regions of wear tracks, microcracks perpendicular to sliding direction are also observed. These results are in good agreement with the result of Cetin [17, 18], who studied dry sliding wear behaviour of a brass against an as-cast ferritic ductile iron and pearlitic ductile iron disc.

The sand cast specimens show wider and deeper grooves under 40 N applied load. However, the grooves of the centrifugally cast specimens are not as wide and deep as those

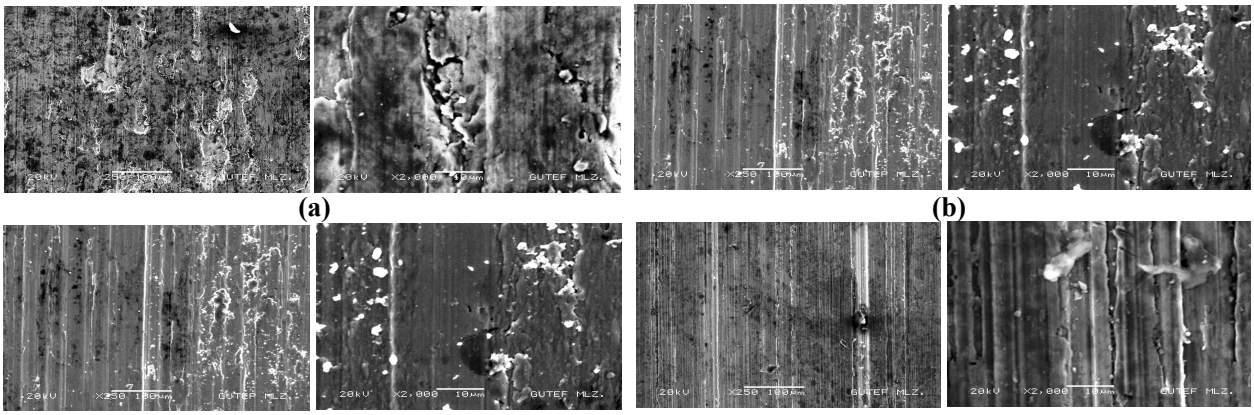

Figure 10. Low (×250) and high (×2000) magnification SEM micrographs of the brasses, which are worn at the 600 m sliding distance, under the 40 N load and at a linear sliding speed of 0.3 m s^{-1} on the various ductile iron disc. (a) and (b) pearlitic disc, (c) and (d) ferritic disc.

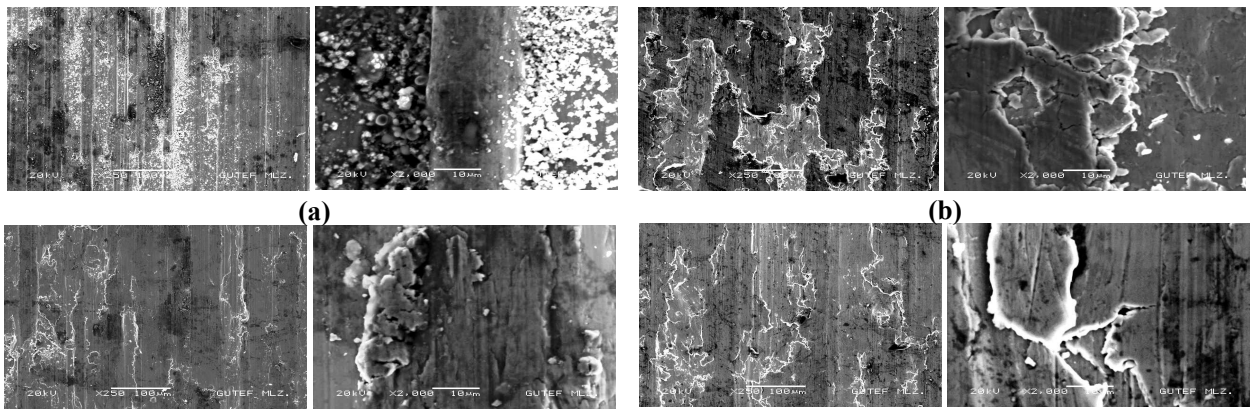

Figure 11. Low (×250) and high (×2000) magnification SEM micrographs of the brasses, which are worn at the 600 m sliding distance, under the 40 N load and at a linear sliding speed of 0.4 m s^{-1} on the various ductile iron disc. (a) and (b) pearlitic disc, (c) and (d) ferritic disc.

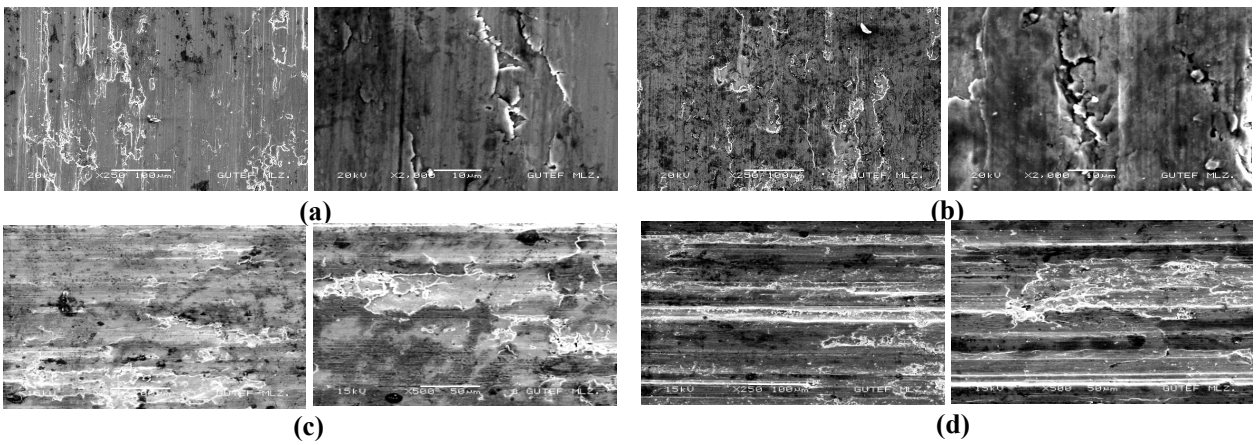

Figure 12. Low (×250) and high (×2000) magnification SEM micrographs of the brasses, which are worn at the 600 m sliding distance, under the 40 N load and at a linear sliding speed of 0.5 m s^{-1} on the various ductile iron disc. (a) and (b) pearlitic disc, (c) and (d) ferritic disc.

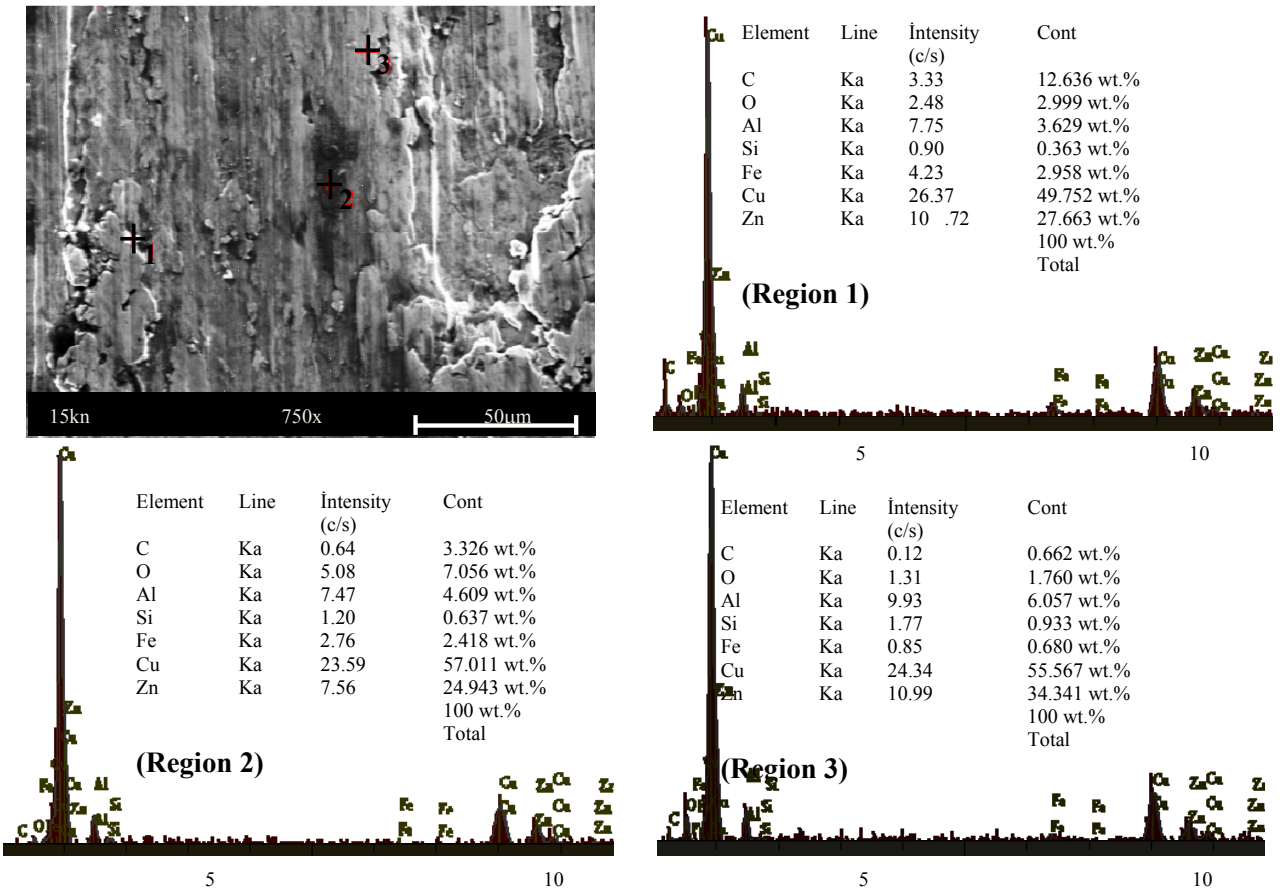

Figure 13. Worn surface SEM and EDAX analysis of centrically cast brass worn under loads of 40 N, at 0.3 m s^{-1} speed and against ferritic ductile iron disc.

of the sand cast specimens under the same load. These can be seen clearly from Figure 10(a), (b) and Figure 11(a), (b). Delamination was also observed on the specimens worn at 0.4 m s^{-1} and 0.3 m s^{-1}and under 40 N applied load, (Figure 11(b), (c) and (d)). Worn surfaces of centrifugally cast specimens (Figure 12) are smoother than those of sand casting specimens. With increasing applied load from 10 N to 40 N, wear surface of the specimens formed shows deeper grooves and local detachment of the pin material as seen in Figure 10(a) and Figure 11(d). As a result, increasing sliding speed increased the deformation for the both materials (Figures 10, 11 and 12). The SEM micrographs of the worn surfaces show a presence of wear debris caused fracture and accumulated into the adhesive wear pits (Figure 10(b) and (c), and Figure 11(a)). At higher specific sliding speeds, presence of material plastic flow and formation of microcracks was obvious (Figure 10(a) and (d), and Figure 11(b)–(d), and Figure 12(a)–(d)). In some regions of wear tracks, microcracks perpendicular to the sliding direction are observed. These microcracks, which indicate the possible wear mechanism as fatigue, were much more apparent for sand cast brass which had low hardness.

Microanalyses of different areas on the worn surfaces of the centrifugally cast and sand cast specimens were analyzed by EDS. Figures 13, 14 and 15 show areas on the worn surfaces of the specimens at high magnification. The EDS spectra taken from three areas namely, region 1 representing a smooth area, region 3 representing a rough and region 2 representing rough/smeared area are shown in Figure 13(a), (b) and (c), respectively. All regions contain mainly copper and zinc. In addition, aluminium, ferrous and carbon are also identified at these regions in Figure 13 but the amount of silicon in the smooth area is much less. This suggests that silicon is not distributed homogeneously on the worn surface in Figure 13 and Figure 14. The EDS result showed that a significant amount of silicon was found on the worn surface of the centrifugally cast specimen. This indicates the transfer of silicon from the ductile iron disc to brass specimen possibly due to the mechanical action during dry sliding (region 3 in Figure 15). Furthermore, from the examination of these photographs of the worn surfaces shown in Figure 11, it is seen that the worn surface of centrifugally cast brass and/or sand cast brass specimens at higher load exhibits more surface damage with distinctly

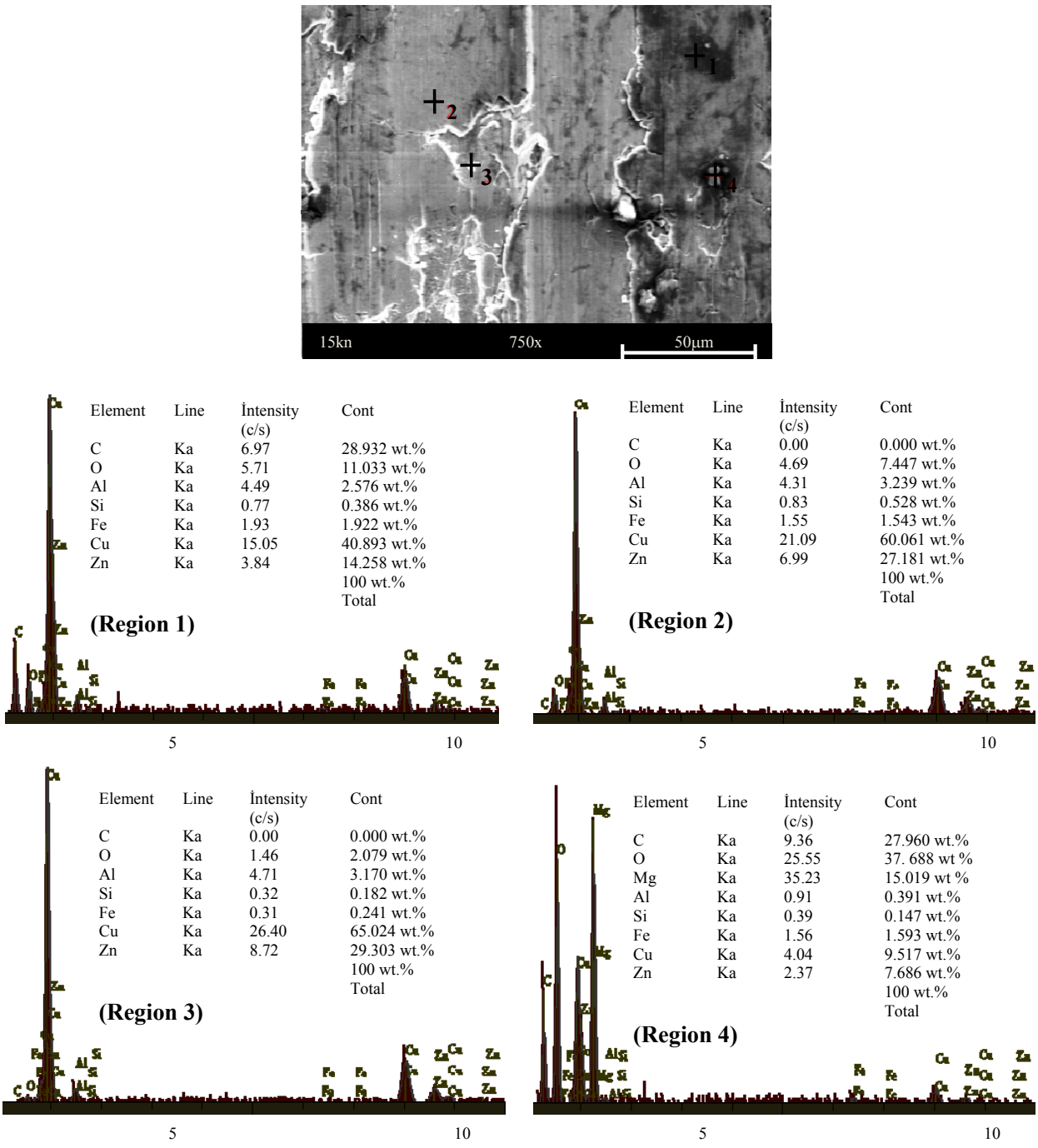

Figure 14. Worn surface SEM and EDAX analysis of centrically cast brass worn under loads of 40 N, at 0.4 m s^{-1} speed and against pearlitic ductile iron disc.

uneven scratches than that at lower load. It is deduced from these scratches that the high load resulted in a high level of wide plastic deformation as mentioned above. Figures 14 and 15 show that increasing sliding speed leads to variation in the worn surface damage. It was reported in [15] that increasing the wear contact load and sliding speed tends to cause high plastic deformation in the subsurface layer of the wear specimens and results in the crack nucleation and crack propagation in the subsurface regions. It is thus thought that in the absence of the formation of any significant protective layer on surface, direct "metal-metal" contact take place between the failed bearing and cast iron counter body. This leads to severe plastic deformation and adhesive wear. The chemical composition of

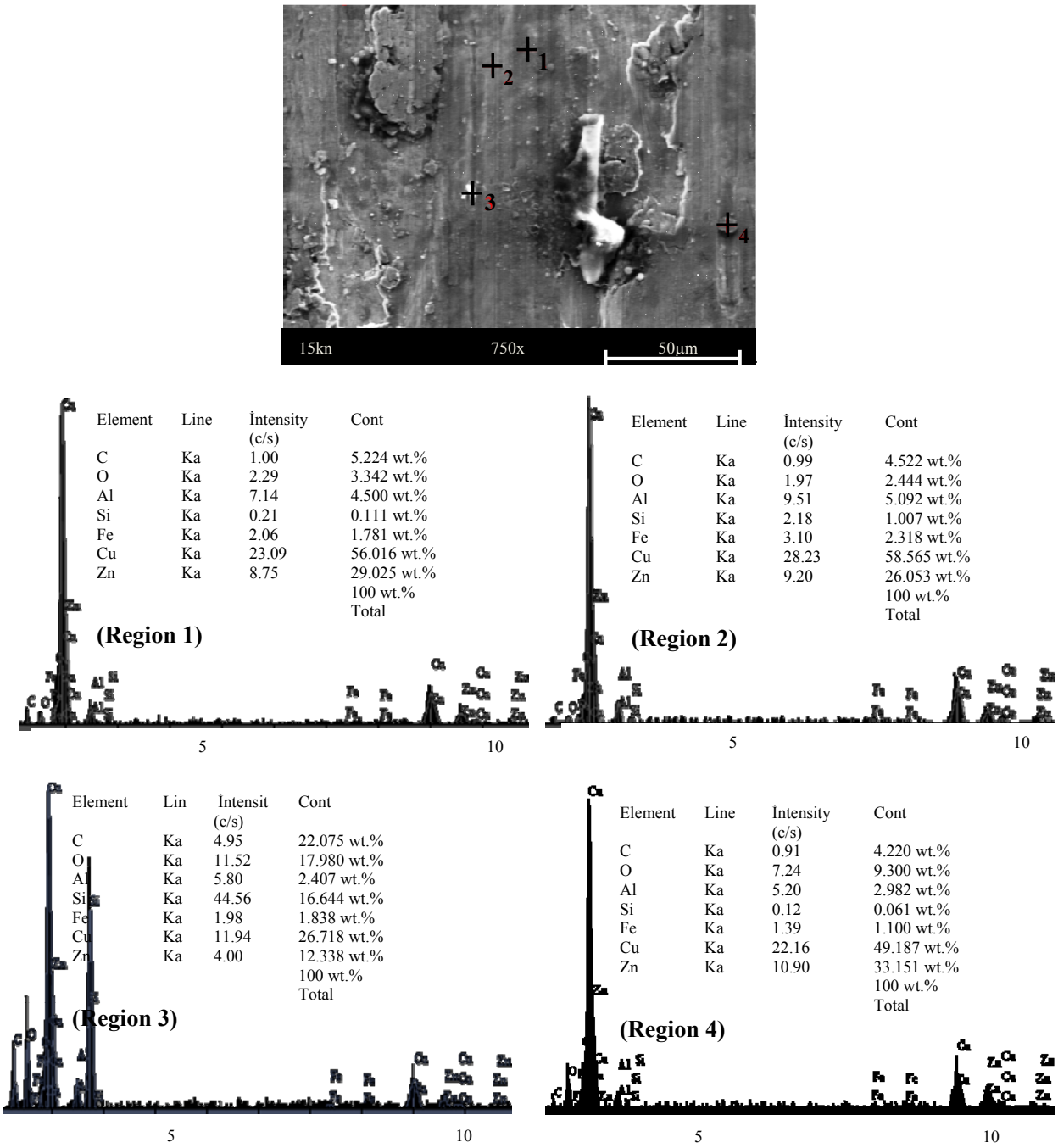

Figure 15. Worn surface SEM and EDAX analysis of centrically cast brass worn under loads of 40 N, at 0.5 m s^{-1} speed and against pearlitic ductile iron disc.

the transferred layer includes magnesium, iron, oxygen and carbon amongst traces of the elements such as Al, Si (region 4 in Figure 14 and Figure 15), which evidently confirms the presence of the wear products from both mating bodies inside the graphite layer. Iron was also found in the patches of dark/gray deposits on the worn surfaces (Figures 13–15). This iron obviously came as debris from the ferritic and pearlitic ductile iron counter body. It can be then reasoned, taking the very low volume rates into consideration that the iron oxidation of the counter body seems to be the prevailing wear mechanisms for the brass/ferritic and pearlitic ductile iron frictional pairs. This layer acts as a protective layer and helps to reduce friction coefficient as well as wear damage. Therefore, the debris from ferritic and pearlitic ductile iron after being embedded in the soft layer form the dark gray patches of deposits on the surface. These

patches of transferred material are believed to stand in relief as "high areas" and reduce metal-metal contact [19]. This is expected to reduce the plastic deformation of the worn surface thereby decreasing the wear damage.

4 Conclusion

In this study, the room temperature dry sliding wear behaviour of brass produced through centrifugal casting and sand casting method was investigated by pin on disc wear tests. The following conclusions can be drawn from this study:

1. The microstructure of the centrifugally cast brass had finer grains than the sand cast brass. Decreasing grain size led to increase in hardness.

2. The wear volume rate of centrifugally cast specimen was found to be less than that of the sand cast specimen under the same tribological conditions.

3. In consistent with the wear results, the wear volume rate of the centrifugally and sand cast specimens is lower for pearlitic ductile iron counterpart compared with for ferritic ductile iron counterpart for all the sliding speeds.

4. At the sliding speed of 0.2 $\mathrm{m\,s^{-1}}$, wear volume rate of the sand casting specimen increased with increasing applied load while wear volume rate of centrifugally cast specimen decreased with increasing applied load.

5. At the sliding speed of 0.3 $\mathrm{m\,s^{-1}}$, wear volume rate of the sand casting specimen decreased with increasing applied load up to 30 N. However, further increase beyond 30 N, increased wear volume rate considerably. On the other hand, wear volume rate of the centrifugally cast specimen decreased with increasing applied load.

6. The experimental results show that the wear volume rate and hardness values of the centrifugally cast brass was found to be better than those of the sand cast brass.

7. The friction coefficient tended to decrease with increase of applied load and sliding speed. The wear volume rate of the centrifugally cast brass increased gradually with the increase of applied load. With increasing sliding speed, the wear volume rate of the centrifugally cast brass decreased in the initial stage and then began to increase. After reaching the maximum wear volume rate at a speed of 0.5 $\mathrm{m\,s^{-1}}$, the volume rate decreased again with further increase in the sliding speed.

8. From the examination of the worn surfaces of wear specimens, it was found that adhesive wear and abrasive wear were the dominant wear mechanisms under dry sliding conditions.

Acknowledgments

The author is grateful to Dr. F. Gul, for providing the necessary facilities. The author is also thankful to Hacioglu Cast Ltd (Karabuk-TR) for providing brass.

References

[1] K. Elleuch, R. Elleuch, R. Mnif, V. Fridrici and P. Kapsa, *Tribology International*, **39** (2006), 290–296.

[2] M. Amirat, H. Zahidi and J. A. Frene, *Proc. I. Mech E Vol. 222 Part J: Journal Engineering Tribology, Special Issue Paper* (2008), 279–290.

[3] B. K. Prasad, *Metal Transactions A,* **A28** (1997), 809–815.

[4] M. M. Haque and A. A. Khan, *J. Materials Science Technology*, **24** (3) (2008), 299–301.

[5] M. Sundberg, R. Sundberg, S. Hogmark, R. Otterberg, B. Lehtinen, S. E. Hornstrom and S. E. Karlsson, *Wear*, **115** (1987), 151–165.

[6] A. Waheed and N. Ridley, *Journal of Materials Science*, **29** (1994), 1692–1699.

[7] H. Mindivan, H. Çimenoglu and E. S. Kayali, *Wear,* **254** (2003), 532–537.

[8] Y. S. Sun, G. W. Lorimer and N. Ridley, *Metallurgical Transactions* A, **20A** (1989), 1989–1199.

[9] S. A. Syed Asif, S. K. Biswas and B. N. Pramila Bai, *Scripta Metallurgica et Materialla*, **24** (1990), 1351–1356.

[10] J. Paulo Davim, *Journal of Materials Processing Technology*, **100** (2000), 273–277.

[11] E. Feyzullahoglu, A. Zeren, and M. Zeren, *Materials & Desing*, **29** (2008), 714–720.

[12] P. J. Blau, *Volume 18 of the ASM Handbook, Friction, Lubrication and Wear Technology* edited by S. D. Henry, 569–577 (1992).

[13] G. W. Stachowiak and A. W. Batchelor, *Engineering Tribology, Vol. 1*, Heineman, Boston (2001).

[14] I. M. Hutchings, *"Tribology: Friction and Wear of Engineering Materials"* Edward Arnold Press, London (1992).

[15] W. X. Qi, J. P. Tu, F. Liu , Y. Z. Yang, N. Y. Wang, H. M. Lu, X. B. Zhang, S. Y. Guo and M. S. Liu, *Materials Science and Engineering A*, **343**(1/2) (2003), 89–96.

[16] M. Boz and A. Kurt, *Tribology International,* **40** (7) (2007), 1161–1169.

[17] M. Cetin, *Technological Applied Sciences,* **4** (3) (2009), 273–279.

[18] M. Cetin, *Technology*, **12** (4) (2009), 227–233.

[19] Q. Ahsan, A. S. M. A. Haseeb, E. Haque and J. P. Celis, *Journal of Materials Engineering and Performance,* **12** (3) (2003), 304–311.